Earthquake Engineering & Structural Dynamics
The Journal of the International Association for Earthquake Engineering

EARTHQUAKE ENGINEERING & STRUCTURAL DYNAMICS
*Earthquake Engng Struct. Dyn.* 2013; **42**:1395–1412
Published online 9 January 2013 in Wiley Online Library (wileyonlinelibrary.com). DOI: 10.1002/eqe.2278

# Validation of ground-motion simulations for historical events using MDoF systems

Carmine Galasso[1,2], Peng Zhong[1], Farzin Zareian[1,*,†], Iunio Iervolino[2] and Robert W. Graves[3]

[1]*Department of Civil and Environmental Engineering, University of California, Irvine, Irvine, CA 92697–2175, U.S.A.*
[2]*Dipartimento di Ingegneria Strutturale, Università degli Studi di Napoli Federico II, Naples, Italy*
[3]*U.S. Geological Survey, Earthquake Science Center, Pasadena Field Office, Pasadena, CA 91106, U.S.A.*

## SUMMARY

The study presented in this paper addresses the issue of engineering validation of Graves and Pitarka's (2010) hybrid broadband ground motion simulation methodology with respect to some well-recorded historical events and considering the response of multiple degrees of freedom (MDoF) systems. Herein, validation encompasses detailed assessment of how similar is, for a given event, the seismic response due to comparable hybrid broadband simulated records and real records. In the first part of this study, in order to investigate the dynamic response of a wide range of buildings, MDoF structures are modeled as elastic continuum systems consisting of a combination of a flexural cantilever beam coupled with a shear cantilever beam. A number of such continuum systems are selected including the following: (1) 16 oscillation periods between 0.1 and 6 s; (2) three shear to flexural deformation ratios to represent respectively shear-wall structures, dual systems, and moment-resisting frames; and (3) two stiffness distributions along the height of the systems, that is, uniform and linear. Demand spectra in terms of generalized maximum interstory drift ratio (IDR) and peak floor acceleration (PFA) are derived using simulations and actual recordings for four historical earthquakes, namely, the 1979 $M_w$ 6.5 Imperial Valley earthquake, 1989 $M_w$ 6.8 Loma Prieta earthquake, 1992 $M_w$ 7.2 Landers earthquake, and 1994 $M_w$ 6.7 Northridge earthquake. In the second part, for two nonlinear case study structures, the IDR and PFA distributions over the height and their statistics, are obtained and compared for both recorded and simulated time histories. These structures are steel moment frames designed for high seismic hazard, 20-story high-rise and 6-story low-rise buildings. The results from this study highlight the similarities and differences between simulated and real records in terms of median and intra-event standard deviation of logs of seismic demands for MDoF building systems. This general agreement, in a broad range of moderate and long periods, may provide confidence in the use of the simulation methodology for engineering applications, whereas the discrepancies, statistically significant only at short periods, may help in addressing improvements in generation of synthetic records. Copyright © 2013 John Wiley & Sons, Ltd.

Received 18 July 2012; Accepted 19 November 2012

KEY WORDS: hybrid broadband simulation; time-history analysis; generalized interstory drift spectra

## 1. INTRODUCTION AND MOTIVATION

For the purposes of building seismic performance assessment and design for target performance via nonlinear dynamic analysis (NLDA), the input earthquake ground motion signals (simply ground motions hereinafter, GMs) can be as follows: (1) actual recorded, eventually scaled GMs from past earthquakes, that is, real records; (2) spectrally matched GMs created by manipulating the frequency

*Correspondence to: Farzin Zareian, Department of Civil and Environmental Engineering, University of California, Irvine, E/4141 Engineering Gateway Building, Irvine, CA, 92697-2175, U.S.A.
†E-mail: zareian@uci.edu

content and intensity of recorded GMs to match a specific response spectrum; (3) artificially (i.e., stochastic-based) simulated GMs; or (4) physics-based simulated GMs. Real records have traditionally been considered the best representation of seismic loading for structural assessment and design, motivating attempts to develop tools for computer-aided code-based real record selection; see [1] for a review. Given the advances in the understanding of fault rupture process, wave propagation phenomena, and site response characterization, simulated GMs of type (4) appear to be one of the viable and attractive alternatives to the very limited amount of recorded GMs, particularly in the nearby field from large earthquakes. The recently released ASCE Standard ASCE/SEI 7-10 [2] explicitly states that, in performing NLDA, 'where the required number of appropriate recorded GM records are not available, appropriate simulated GM shall be used to make up the total number required.'

The current state-of-the-art simulation procedures are based on a hybrid broadband approach that combines deterministic low-frequency synthetics up to a maximum frequency of typically 1–2 Hz with high-frequency stochastic simulation above this upper cutoff frequency (e.g., [3]). However, to date, simulated GMs have not found significant practical application because of a general sense that they have not been adequately validated and they are not yet readily available to engineers.[‡] This latter issue traditionally favored the use of spectrum-matched accelerograms [4], either artificially generated or obtained through modification of real waveforms in time and/or frequency domains, even if they have not yet been extensively validated.

The study presented in this paper addresses the issue of engineering validation of Graves and Pitarka's (2010) hybrid broadband GMs simulation methodology with respect to some well-recorded historical events and considering the response of multiple degrees of freedom (MDoF) systems. This validation encompasses detailed assessment of how similar is the seismic response potential due to hybrid broadband records compared with the seismic response potential due to real records. A concurrent study by Galasso *et al.* [5], based on spectral analysis of both elastic and inelastic single degree of freedom (SDoF) systems, shows that seismic demands of SDoF systems subjected to simulated and recorded motions are generally comparable. However, for some structural systems, the inelastic response to simulated accelerograms may produce median demands that appear different from those obtained using corresponding recorded motions. In the case of peak deformation response, these discrepancies are likely due to differences in the elastic spectral shape, whereas the differences in terms of cyclic response can be explained by some energy parameters of GM (i.e., duration-related). Assessment of the results using formal statistical hypothesis tests indicates that in most cases, the differences found are not statistically significant, increasing the confidence in the use of simulated motions for engineering applications.

This study aims at taking a step forward and trying to understand if simulated GMs are comparable to real records in assessing the seismic behavior of MDoF structural systems where higher modes may substantially contribute to the total response. For such structural systems, whose fundamental period can be long, the traditional SDoF spectral analyses may significantly underestimate local structural deformation. Furthermore, the displacement response obtained from spectral ordinates can only provide an overall measure of lateral deformation of the structure and do not take into account concentration of demand in certain stories that may occur in actual buildings. Higher modes of vibration also contribute significantly to the acceleration demands in buildings—a response parameter that recent studies show significant to nonstructural damage and monetary loss (e.g., [6] and [7]).

The presented study investigates the validity of hybrid broadband GM simulation methodology using both conceptual (or generalized) MDoF systems and nonlinear building models. The conceptual MDoF systems considered in the first part of this study are modeled as equivalent continuum structures that consist of a flexural cantilever beam coupled with a shear cantilever beam (both with uniform mass distribution), for example, [8]. Such a generalized model is a viable tool to approximate real buildings, especially tall structures, ranging from moment-resisting frames to shear-wall systems, and for which

[‡]To overcome this latter limitation, the recently released Southern California Earthquake Center (SCEC) Broadband Platform (http://scec.usc.edu/research/cme/groups/broadband) provides scientists and engineers with a suite of tools to compute broadband synthetic ground motions, including the effects of heterogeneous rupture propagation and nonlinear site effects.



DOI: 10.1002/eqe

the higher-mode contributions may become important. Moreover, it permits obtaining estimates of seismic response of multistory buildings with only three parameters: $T_1$, $\xi$, and $\alpha$, which are the fundamental period, the critical damping ratio at the first mode of vibration, and a nondimensional quantity controlling the degree of contribution of flexural and shear deformations in the MDoF's total deformation, respectively. By varying $\alpha$, one can control relative contributions of the two types of deformation on the total response, providing the opportunity to account for a wide range of modes of deformation that represent more closely those of multistory buildings. Parameters such as the fundamental period and the variation of stiffness along the height of the systems can also be parameterized. Conceptual MDoF systems in the manner described here inherits some of the limitations and assumptions of modal analysis, such as assuming a linear elastic behavior and a classical damping. Hence, the method is aimed at the estimation of seismic demands at performance levels in which the building is expected to respond elastically or with very limited levels of nonlinearity, such as conventional buildings subjected to moderate earthquake GMs or critical facilities during severe earthquakes.

To overcome the limitations related to the use of conceptual MDoF systems, two building models, whose structural elements can properly capture the nonlinear behavior, are used for the validation process. These structures are a 20-story high-rise building and a 6-story low-rise building similar to many steel moment frame (SMF) structures in Los Angeles [9], with SMFs and ductile post-Northridge welds. Lumped plasticity frame models are developed with the most current knowledge of nonlinear modeling techniques and component properties, and are subjected to recorded and simulated GMs.

For both elastic and inelastic systems, seismic demands in terms of interstory drift ratio (IDR) and peak floor acceleration (PFA) are derived for four historical earthquakes. The final goal is to address, on a statistical basis, whether simulated GMs are biased in terms of median MDoF response characteristics in comparison with real records. Intra-event variability of response to recorded and simulated GMs is also investigated. Finally, hypothesis tests on selected samples, taking the approach of [10], are carried out to assess the statistical significance of the results.

## 2. DESCRIPTION OF SYNTHETIC AND REAL GROUND MOTIONS DATASETS

Graves and Pitarka [3] developed and validated (in terms of elastic spectral ordinates) a hybrid broadband (0–10 Hz) GM simulation methodology that uses simple kinematic representation of slip distribution and rupture velocity on the fault surface. More specifically, to simulate broadband time histories, the GMs are computed separately in short-period and long-period ranges and then combined into a single broadband time history through a matching filter. This is because GMs fundamentally have different characteristics in these two period ranges. At long periods (longer than 1 s, i.e., $f \leqslant 1$ Hz,), strong GMs are deterministic in the sense that rigorous seismological models are capable of matching not only the spectral amplitudes but also the recorded waveforms, once the rupture model of the earthquake and the seismic velocity structure of the region surrounding the earthquake are assumed. At short periods (shorter than 1 s, i.e., $f > 1$ Hz), strong GMs become increasingly heterogeneous in nature. Seismological models are generally capable of matching the spectral ordinates of the short-period GMs but are generally not capable of matching the recorded waveforms. The transition from deterministic to stochastic behavior appears to be due to a transition from coherent source radiation and wave propagation conditions at long periods to incoherent source radiation and wave propagation conditions at short periods.

The local geology affects both the amplitude and shape of response spectra. In order to account for site-specific geologic conditions in the final broadband response, period-dependent, nonlinear amplification factors are applied to the simulated time histories. These amplification factors are based on the 30-m travel-time averaged shear-wave velocity ($V_{S,30}$) at the site of interest and were developed using equivalent linear site response analysis as implemented in the GM prediction equation of Campbell and Bozorgnia [11]. This formulation is chosen because it employs separate terms for deep-basin amplification (which is explicitly included in the low-frequency simulation) and local site-specific amplification.



DOI: 10.1002/eqe

For the validation process addressed in this paper, four historical earthquakes, modeled by using the technique described in [3], are used: 1979 $M_w$ 6.5 Imperial Valley, 1989 $M_w$ 6.8 Loma Prieta, 1992 $M_w$ 7.2 Landers, and 1994 $M_w$ 6.7 Northridge. The earthquake-specific input parameters used in the simulation process are seismic moment, overall fault dimensions and geometry, hypocenter location, and a smoothed representation of the final slip distribution. All other required source parameters (e.g., rupture propagation time, rise time, slip function, and fine-scale slip heterogeneity) are simulated using the scaling relations presented in [3]. Furthermore, the methodology provides a framework to generate rupture descriptions for future earthquakes, as demonstrated in [12].

For each earthquake simulation, the model region covers a wide area surrounding the fault including many strong motion recording sites available in the *Next Generation Attenuation* database (http://peer.berkeley.edu/peer_ground_motion_database): 33 for Imperial Valley, 71 for Loma Prieta, 23 for Landers, and 133 for Northridge earthquake. Only a limited number of these sites are used here, that is, those with a usable bandwidth of the real records exceeding 0.1 s–8 s, yielding a total of 126 sites (Figure 1), while the analysis and results presented refer to structures with fundamental periods less than 6 s. With this approach, it is possible to cover a realistic range of initial linear elastic fundamental vibration periods.

## 3. VALIDATION VIA GENERALIZED LINEAR MDoF SYSTEMS

The conceptual model used in the first part of this study is schematically shown in Figure 2. It consists of a flexural cantilever beam and a shear cantilever beam deforming in bending and shear configurations, respectively (e.g., [8]). The two beams are assumed to be connected by an infinite number of axially rigid members that transmit horizontal forces; thus, the flexural and shear cantilevers in the combined system undergo the same lateral deformation at all heights. Floor mass and lateral stiffness are assumed

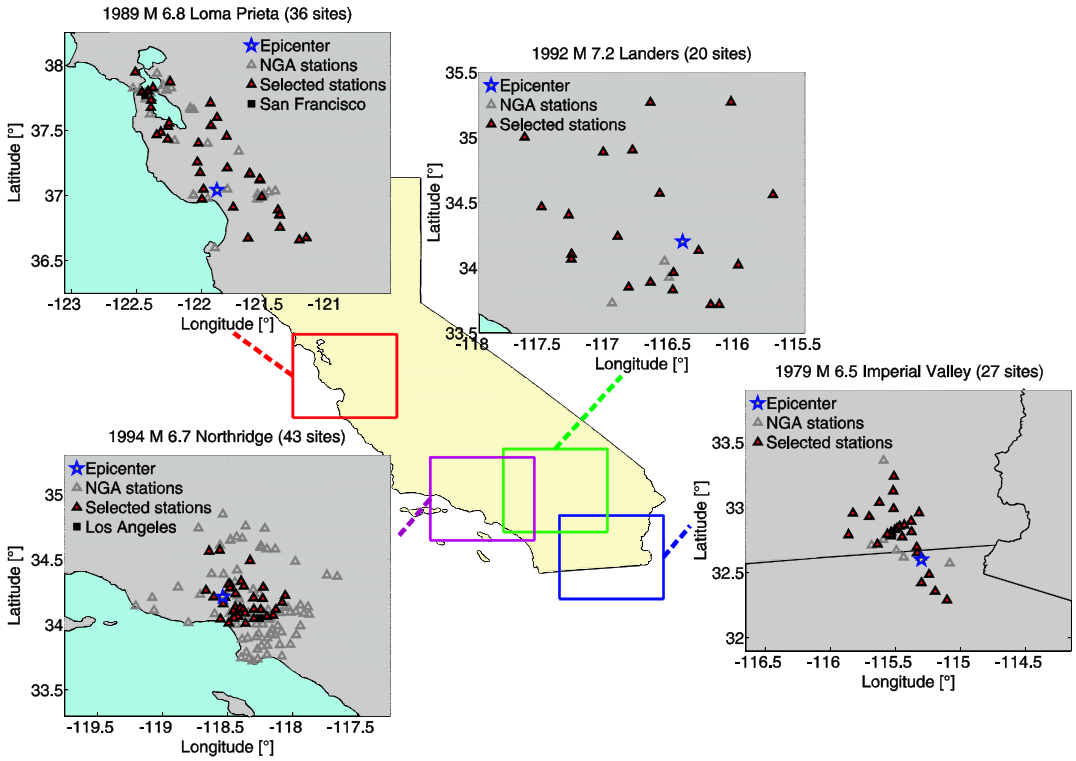


Figure 1. Maps of the considered earthquakes. The star is the epicenter and the gray triangles are recording stations of the NGA database for which the simulations are available. The red triangles are recording stations considered in this study. San Francisco and Los Angeles are also indicated on the map (black squares).



DOI: 10.1002/eqe

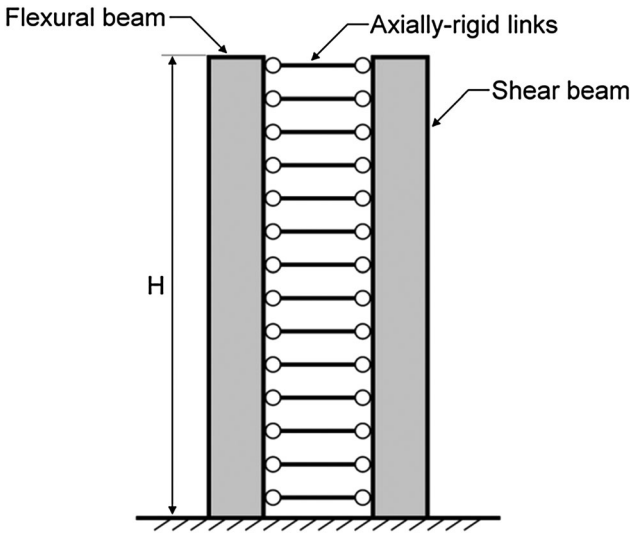


Figure 2. Simplified model used in deriving the generalized interstory drift spectrum (adapted from [8]).

to remain constant along the height of the building, although modifications for nonuniform mass and stiffness distribution over the height of the building have been proposed and are considered in the following.

Previous studies have provided closed-form solutions for the fourth-order partial differential equation describing the combined shear and flexural beams for the following cases: (1) lateral static loading to approximate the maximum roof and interstory drift demands of first-mode dominated structures [8]; (2) computing the approximate dynamic structural behavior (in terms of lateral displacements and PFAs) by using up to the first three modes of vibration [6]; (3) and estimating generalized drift spectra [13]. Evaluation of the results presented in the aforementioned studies indicates that this analysis tool provides relatively good results not only in terms of peak values of response parameters but also, in most cases, for response history results.

The power of the conceptual MDoF system described here is in its simplicity; in fact, mode shapes, modal participation factors, and the ratio of the period of vibration of higher modes to the fundamental period are fully defined by only three parameters: $T_1$, $\xi$, and $\alpha$, namely the fundamental period, the critical damping ratio at the first mode of vibration, and the lateral shear to flexural stiffness ratio [13], respectively. In particular, Equation (1) gives $\alpha$, where $H$ is the total height of the building, $GA$ is the shear stiffness of the shear beam, and $EI$ is the flexural stiffness of the flexural beam.

$$\alpha = H\sqrt{\frac{GA}{EI}} \tag{1}$$

The dimensionless parameter $\alpha$ controls the degree of participation of flexural and shear deformations in the total deformation of the simplified model. Miranda and Reyes [14] indicate that lateral deflected shapes of buildings, whose lateral resisting system consists only of structural walls, can usually be approximated by $\alpha$ between 0 and 2. The same study indicates that for buildings with dual lateral resisting systems consisting of a combination of moment-resisting frames and shear walls or a combination of moment-resisting frames and braced frames, values of $\alpha$ are typically between 1.5 and 6. For buildings whose lateral resisting system consists only of moment-resisting frames, values of $\alpha$ are typically between 5 and 20.

As an example, the curves in Figure 3(a) show the normalized fundamental modal shapes and corresponding interstory drift as a function of the nondimensional height $z = x/H$ for three considered $\alpha$ values (i.e., 0.1, 8, and 30; these values are used in the rest of the study). In extreme cases when the structure behaves as a flexural cantilever beam ($\alpha = 0.1$) or in the buildings where lateral shear deformations dominate over lateral flexural deformations ($\alpha = 30$), the maximum IDR occurs at the



DOI: 10.1002/eqe

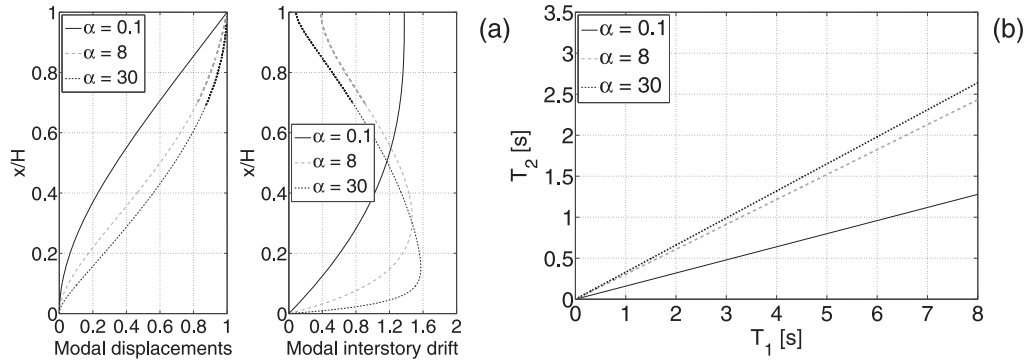


Figure 3. (a) Dependence of the lateral deformation (in terms of modal displacement and modal interstory drift) on $\alpha$ for the first mode. (b) Dependence of the second-mode period ($T_2$) on the first-mode period ($T_1$) for different $\alpha$ values.

top or near the ground story, respectively (assuming that the structural behavior is dominated by the first mode of vibration). Figure 3(b) shows the relationship between the fundamental period of buildings and second-mode period. Note that in the case of $\alpha = 0.1$, for structures with fundamental period less than 6 s, the second-mode period is less than 1 s, which is in the semistochastic part of the hybrid broadband simulation. In the other two cases (i.e., $\alpha = 8$ and 30), this happens only for a structure with a fundamental period less than about 3 s. This confirms the importance of considering higher modes effects for comparison of seismic demands due to simulated and recorded GMs, which are not considered in simpler validation procedures that only employ elastic spectral ordinates at the fundamental period of the structure.

Note that, while assuming the mass to remain constant along the height of buildings is reasonable in most cases, the building's lateral stiffness does not remain constant along the height except for low-rise buildings (e.g., less than three stories). Miranda and Taghavi [6] provided expressions to compute the dynamic characteristic of non-uniform buildings, although they concluded that in many cases, using the dynamic characteristics of uniform models could provide reasonable approximations to the dynamic characteristics of non-uniform models. In the simplified model used in this study, the base of the model has been assumed to be fixed; foundation flexibility and torsional deformations are neglected.

### *3.1. Description of the considered systems and demand measures*

In order to study the dynamic response of a wide range of buildings, a number of simplified continuum systems are selected including the following: (1) 16 (fundamental) oscillation periods, simply $T_1$ hereafter, between 0.1 and 6 s; (2) three shear to flexural deformation ratios, $\alpha$, to represent respectively shear walls structures ($\alpha = 0.1$), dual systems ($\alpha = 8$), and moment-resisting frames ($\alpha = 30$); and (3) two stiffness distributions along the height of the systems, that is, uniform and linear. In the latter case, the ratio of the lateral stiffness at the top of the structure to the lateral stiffness at the base is assumed equal to 0.25. The period range is sampled with a 0.1s step from 0.1 to 0.5 s, with a step of 0.25 s between 0.5 and 1 s, with a step of 0.5 s between 1 and 5 s, and with a step of 1 s between 5 and 6 s.

It is general belief that the engineering demand parameter (EDP) that is best correlated with seismic damage is the peak IDR, defined as the difference in lateral displacements between two consecutive floors normalized by the interstory height. Similarly, damage to contents and many nonstructural components are primarily related to PFA and to floor acceleration spectra (to follow).

The generalized demand spectra in terms of maximum IDR (MIDR; i.e., the maximum time-peak rotation $\theta(z,t)$ over the height of the building) is derived as shown in Equation (2). For a given fundamental period of vibration, the total height of the model is computed using the relationship (in metric units) suggested for steel moment-resisting frames in ASCE 7-2010 [2] (Equation (3)). To derive the system demands, some assumptions were taken: (1) uniform distribution of mass along the height of the building; (2) equal damping ratios of 5% for all modes; and (3) only the first six modes of vibration are considered so that the sum of their effective modal masses contains more than 90% of the system total mass.



DOI: 10.1002/eqe

$$\mathrm{MIDR} = \max_{\forall t,z} |\theta(z,t)| \tag{2}$$

$$T = 0.0724H^{0.8} \rightarrow H = \sqrt[0.8]{\frac{T}{0.0724}} \tag{3}$$

### 3.2. Results and discussions

A direct comparison of response statistics is appropriate because the simulated datasets were developed to match exactly the same earthquakes and site conditions (i.e., at the same stations) of the actual recordings. GM pairs (recorded and simulated) selected for each earthquake are used as input for the seismic analysis of the MDoFs discussed in the previous section; a total of about 24,000 analyses are performed. Only horizontal components of GMs (i.e., NS, north–south; EW, east–west) are used. The spectral responses for the two horizontal components at each station is computed and then combined into an 'average' spectral response by using the geometric mean.

For each earthquake, the median value of the MIDR (i.e., the exponential of the mean of the natural log of the MIDR across all the available stations in the case of lognormal distribution for MIDR) for simulated records divided by the corresponding median value for the recorded dataset is computed and plotted across the considered period range (for different values of $\alpha$). A ratio above unity, if statistically significant, means systematic overestimation (i.e., bias) of the response by simulation and below unity means underestimation. More specifically, a deviation above unity of the considered ratio indicates that the synthetic records in that dataset tend to produce, on average, systematically more intense seismic demands in terms of MIDR than those by real records. Conversely, deviations below unity indicate that the simulated records tend to be, on average, more benign, in terms of MIDR, than those in nature.

In order to provide a measure of inherent variability in the simulations compared to that of real GMs, the ratio of standard deviation of MIDR (in terms of the natural log of the data, approximately equal to the coefficient of variation of non-log data in the case of lognormal distribution) for recorded and simulated GMs was plotted as a function of MDoF fundamental period and $\alpha$. A line above unity approximately means more record-to-record variability around the mean produced by synthetic GMs, whereas the opposite is true for a line below unity.

*3.2.1. Comparison between statistical measures of generalized MIDR spectra.* In general, the generalized MIDR spectra from simulated waveforms agree reasonably well with those from the observed waveforms. The median value of the MIDR for the simulated records ($\mathrm{MIDR_{sim}}$) divided by the median value of the MIDR for the recorded dataset ($\mathrm{MIDR_{rec}}$) is plotted across the period range of 0.1 to 6 s in Figure 4(a) for the three considered $\alpha$ values for the Imperial Valley earthquake. Similarly, Figure 4(b) shows, for the same event, the ratio of the standard deviation of MIDR (log of the data) for synthetic GMs divided by the standard deviation of MIDR (log of the

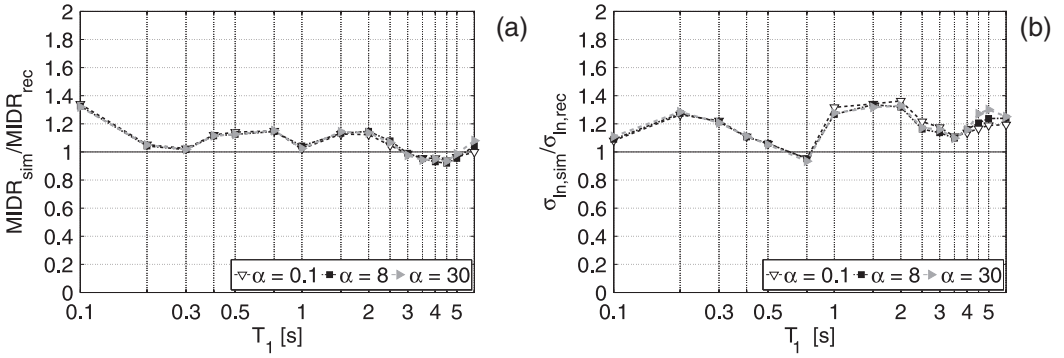


Figure 4. Ratios of the medians (a) and log-standard deviations (b) of the generalized MIDR spectra for simulated GMs to the corresponding quantity computed for the recorded GMs for the Imperial Valley earthquake.



DOI: 10.1002/eqe

data) for recorded GMs. Figure 4 refers to uniform stiffness distribution along the height of the systems. Figures 5–7 are developed in the same fashion as Figure 4, however, for Loma Prieta, Landers and Northridge, respectively. Results for the case of linear stiffness distribution along the height of the systems are not shown; however, similar observations can be drawn for it.

With the simplified model introduced in the previous sections, bias (i.e., the departure of the considered ratios from unity) in the elastic response of conceptual MDoF systems is earthquake-dependent, period-dependent, and slightly $\alpha$-dependent. Deviations seem to be concentrated in the zone of semistochastic simulation (at very short periods) and around 2 s. The observed differences

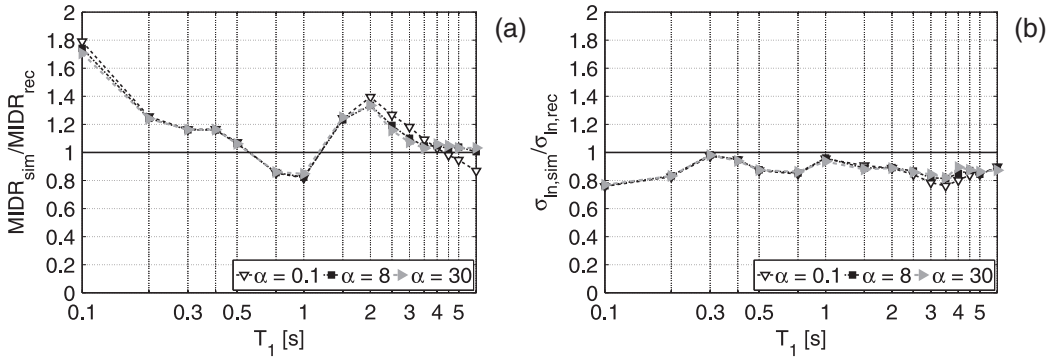


Figure 5. Ratios of the medians (a) and log-standard deviations (b) of the generalized MIDR spectra for simulated GMs to the corresponding quantity computed for the recorded GMs for the Loma Prieta earthquake.

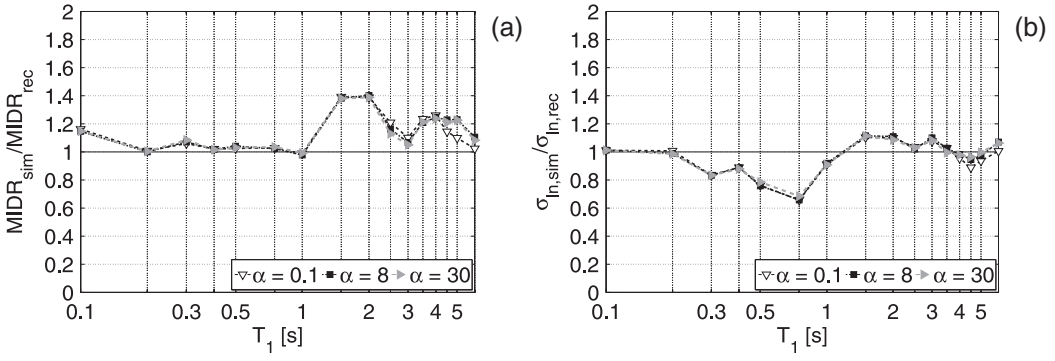


Figure 6. Ratios of the medians (a) and log-standard deviations (b) of the generalized MIDR spectra for simulated GMs to the corresponding quantity computed for the recorded GMs for the Landers earthquake.

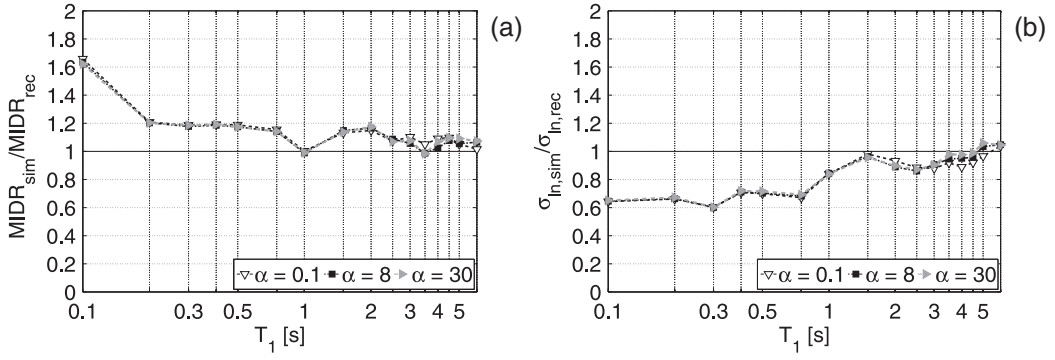


Figure 7. Ratios of the medians (a) and log-standard deviations (b) of the generalized MIDR spectra for simulated GMs to the corresponding quantity computed for the recorded GMs for the Northridge earthquake.



DOI: 10.1002/eqe

at given periods are likely due to systematic differences in the average shape around those periods of the linear response spectra generated by synthetic and by real GMs (to follow). For Loma Prieta and Northridge, both characterized by buried ruptures, the comparisons in Figures 5 and 7 produces very similar results; Imperial Valley and Landers are both surface events with similar results.

Except for one out of four historical events studied here, that is, Imperial Valley, the log-standard deviations of the generalized MIDR spectra of the real records are generally larger compared with the simulated GMs, particularly at the shorter periods. This trend of relatively low intra-event variability in the simulations, especially at short periods, has been noted previously in [15]. Seyhan *et al*. [16] have recently proposed a revision to the simulation approach that incorporates greater stochastic variability in the high-frequency portion to address this issue, although this revision has not yet been applied to the simulations considered in the current analysis.

In the case of the Imperial Valley event, the log-standard deviation of the response to simulated records is larger than that to recorded ones across the entire period range (the considered ratio is almost constant and above the unity). At long periods, this can be attributed to the presence in the simulated dataset of GMs featuring strong coherent velocity pulses [3] and then large elastic response. The reason for this increased variability is that the deterministic approach can create strong spatial variability in the near fault GMs because of the characteristics of the rupture and also the 3D geology (if that is included). This not only is limited to strong coherent pulses in the forward rupture direction but also includes less coherent motions in the neutral or backward directivity direction. In addition, at low frequencies, the deterministic simulations are also much more sensitive to the distribution of slip on the fault. Because of the nature of the randomness in the stochastic approach, all these features tend to be homogenized (e.g., the stochastic approach uses an averaged radiation pattern for all sites), and thus, the spatial variability in the near fault region is generally diminished relative to the deterministic approach and to the recorded GMs. However, in the case of Imperial Valley, the relative complexity of the regional velocity structures where this event occurred [3] and, probably, some inadequacies in the velocity model used in the simulation (and the assumed inelastic attenuation function) result in large variability of the response because of simulated GMs also at short periods.

*3.2.2. Comparison in terms of floor acceleration spectra.* In this section, focus is made on acceleration demands of two case study tall buildings subjected to simulated and recorded GMs. In particular, floor acceleration spectra for four different locations along the height are obtained and plotted in terms of ratio between median of structural response to simulated and recorded GMs. Floor accelerations spectra allow the estimation of accelerations demands at different frequencies. This information is useful, for example, for acceleration-sensitive nonstructural components (characterized by a weight smaller than the weight of the building) for which the PFA is not enough.

The first structure (SF48) is a pyramidal-shape 257-m tall building in San Francisco, built in 1972; its lateral resisting system consists of interior and exterior steel moment-resisting frames. It was shaken by the 1989 Loma Prieta earthquake. The second structure considered (LA52), built in 1990, is in Los Angeles and has 52 stories above ground; it has a square floor plan and the lateral resisting system, in both directions, consists of concentrically braced steel frames at the core with outrigger moment-resisting frames in the exterior. This structure was hit by several earthquakes, including the 1994 Northridge event.

Both structures are instrumented, allowing the estimation of the parameters that are needed in each direction to perform the simplified analysis; see [17] for details. The parameters used for each of the buildings are listed in the last three columns of Table I (the damping ratio of all modes is assumed to be the same in order to reduce the number of parameters required to fully define the simplified model to three); also, in this case, six modes for each direction of the motions are considered for both structures. For both buildings, despite some important reductions in lateral stiffness that exist as height increases (especially for the SF48 building), Reinoso and Miranda showed that the simplified model is able to capture very well the variation of seismic demands along the height derived from recorded data. Given the different properties of the two buildings in each horizontal direction, separate comparisons for each component of GM (i.e., NS, north–south; EW, east–west) are performed.



DOI: 10.1002/eqe

Table I. Buildings and events used in this study (adapted from [17]).

| ID | Location | Stories | Earthquake | Ep. Dist. (km) | Comp. | $T_1$ (s) | $\alpha$ | $\xi$ |
|---|---|---|---|---|---|---|---|---|
| SF48 | San Francisco | 48 | Loma Prieta | 97 | NS | 3.57 | 25.0 | 1.2 |
| | | | | | EW | 3.70 | 25.0 | 1.5 |
| LA52 | Los Angeles | 52 | Northridge | 31 | NS | 5.90 | 9.8 | 1.0 |
| | | | | | EW | 6.20 | 6.9 | 1.5 |

The median value of floor accelerations for the simulated records ($acc_{sim}$) divided by the median value of floor accelerations for the recorded dataset ($acc_{rec}$) is plotted across the period range of 0.1 to 6 s in Figure 8(a) for the SF48 building subjected to the Loma Prieta event and in Figure 8(b) for the LA52 building shaken by the Northridge earthquake. In both plots, four different locations along the height of the building, expressed in terms of nondimensional height $z$, are considered, that is, 25%, 50%, 75%, and the roof. The considered ratios seem to be slightly dependent on the $z$ values in all the period range and on the GM component. The results in Figure 8 confirm the results found in terms of MIDR for the Loma Prieta and Northridge earthquakes (Figure 5 and 7, respectively): simulated GMs tend to significantly overestimate the acceleration demands in the short-period part of the spectra. In the moderate-period to long-period ranges, the simulation matches well the acceleration demands produced by recorded GMs, and the bias is close to zero for a wide period range. Also, in this case, it is evident that the simple validation of GM simulations by using elastic spectral ordinates may not suffice.

### *3.3. Hypothesis tests*

Parametric hypothesis tests are performed to quantitatively assess the statistical significance of the results found in median response (for each oscillation period, each $\alpha$ value, and each earthquake) to recorded and simulated GMs. The intention is to assess whether the ratios presented in the previous section differ systematically from unity. Hypothesis tests are performed assuming a lognormal distribution for both EDPs, that is, MIDR and PFA. This distribution assumption is checked with the Shapiro-Wilk [18] test and could not be rejected at a 95% significance level.

Taking the same validation approach in [10], the hypothesis is whether the median MIDR (and the median PFA) for simulated GMs is equal (i.e., null hypothesis) or not (i.e., alternate hypothesis) to those from recorded GMs. To this aim, a two tails Aspin-Welch [19] is considered. The test statistic employed is reported in Equation (4), in which $z_x$ and $z_y$ are the sample means, $s_x$ and $s_y$ are the sample standard deviations, and $m$ and $n$ are the sample sizes (in this case, always equal for each earthquake). The test statistic, under the null hypothesis, has a Student $t$-distribution with the number of degrees if freedom given by Satterthwaite's approximation [20].

$$t = \frac{z_x - z_y}{\sqrt{\frac{s_x^2}{n} + \frac{s_y^2}{m}}} \tag{4}$$

An $F$-test (e.g., [21]) for normally distributed data has been performed in terms of comparison between variances (in log terms), for the two datasets (recorded and simulated) corresponding to each earthquake; in this case, for each structural system, the null hypothesis is that the variance of structural response (i.e., MIDR and PFA) for simulated GMs is equal to the variance from recorded GMs.

Hypothesis tests results for MIDR spectra are summarized in Figure 9. To draw conclusions, percentages of hypothesis tests rejections assuming a 95% significance level (i.e., choosing a I-type risk, $\alpha_I$ equal to 0.05) are shown in Figure 9 for each pair ($T$, $\alpha$). In computing these percentages, all the earthquakes and structural models are considered together, yielding a total of eight cases. On the basis of Figure 9, tests have shown a statistical significance of the bias of simulated record in terms of MIDR ratio only for very short-period structures and around 2 s for all the considered $\alpha$ levels. These results confirm the considerations based on the visual inspection of Figures 4–7.



DOI: 10.1002/eqe

Similarly, tests have shown a statistical significance of the bias of simulated record in terms of PFA. This significance goes up to a period of 0.5 s in the case of SF48 building and up to 1.0 s in the case of LA52 building, confirming the derived conclusions on bases using visual inspection of Figure 8.

To investigate the possible sources of the found differences in the short-period range, for each of the four events considered in this study, the median value of the elastic displacement spectral ordinates for the simulated records divided by the median of that parameter for the recorded dataset is computed and plotted across the considered period range in Figure 10. From inspecting the graphs in Figure 10, it emerges that not only the median spectral amplitudes but also the spectral shapes for simulated GMs can be different from the median response spectrum of real recordings. In fact, in the median ratios shown in Figure 10, any trend across the periods that departs from a horizontal line suggests that the elastic spectra generated by the synthetic model have, on average, a different shape than those produced by nature. The difference in spectral shape is large especially for Loma Prieta and Landers events, for a wide range of periods. These differences in terms of spectral shape have an influence on the multi-mode response of the considered systems. In fact, given the contribution of higher modes, the displacement and acceleration demands of an MDoF system (i.e., MIDR and PFA) are dependent on the frequency content of the record in a fairy large bandwidth, including smaller periods, and not only in the neighborhood of the first period of vibration. Therefore, even if hypothesis tests do not confirm the differences in spectral amplitudes to be statistically significant, the differences in spectral shape leads to statistical significant differences in terms of MIDR and PFA, confirming the need for an engineering validation beyond the simple elastic SDoF analysis.

### *3.4. Sensitivity of ground motion simulations to source-to-site distance and site conditions*

In this section, a closer look at the influence of source-to-site distance, and site conditions, on the ratios of the medians and log-standard deviations of the generalized MIDR spectra for simulated and recorded GMs is presented. Specifically, the considered variables are the closest distance to the fault, $D$ (in km), and the shear-wave velocity in the upper 30 m, $V_{S,30}$.

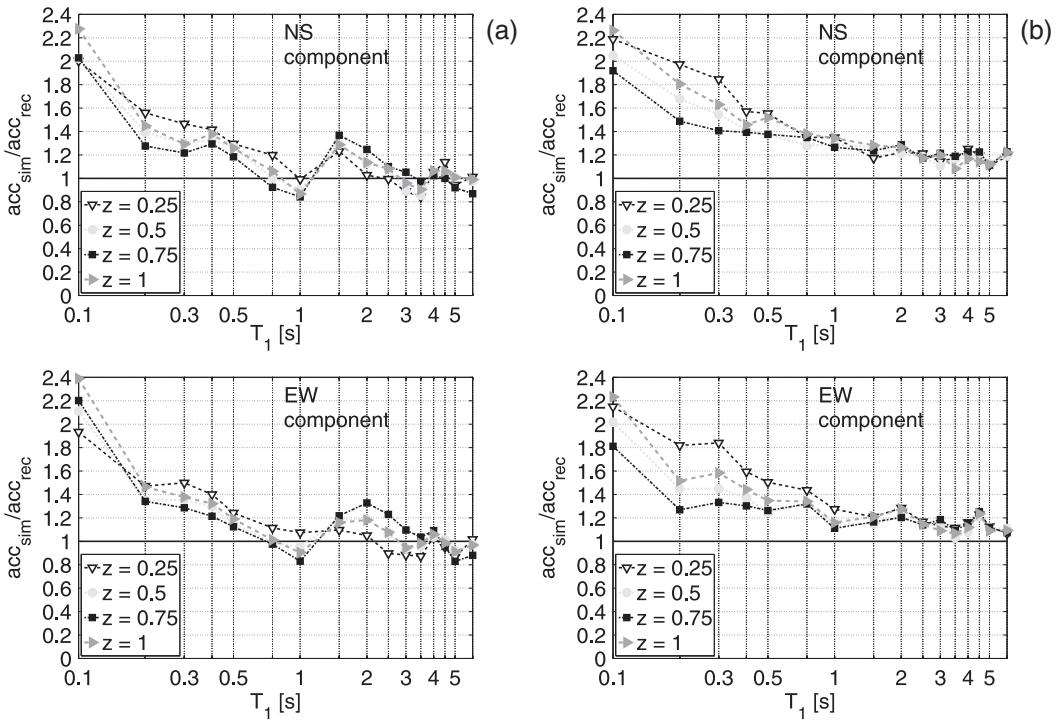


Figure 8. Ratios of the medians of the floor accelerations spectra for simulated GMs to the corresponding quantity computed for the recorded GMs for the (a) SF48 buildings and (b) LA52 building.



DOI: 10.1002/eqe

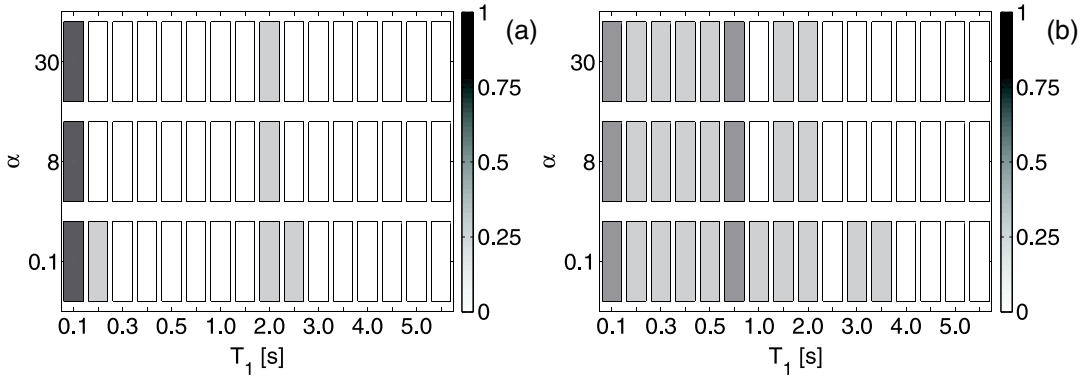


Figure 9. Percentage of hypothesis test rejections ($\alpha_I = 0.05$) for MIDR: (a) equality of medians and (b) equality of variances.

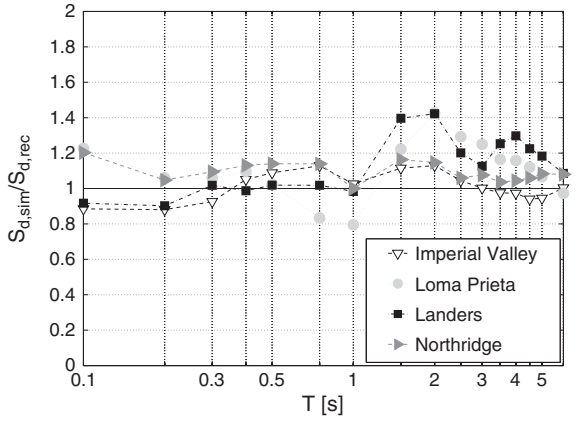


Figure 10. Ratios of the medians of the elastic displacement spectra for simulated GMs to the corresponding quantity computed for the recorded GMs.

*3.4.1. Effect of distance to the source.* Two subsets of the recording stations for the Northridge earthquake representing two different distance ranges, that is, $D \leqslant 20$ km (with 20 GMs) and $D > 20$ km (with 23 GMs), are assembled. Northridge earthquake was selected because it is characterized by the largest number of stations. Figure 11(a) shows the ratio of the median spectrum in terms of MIDR from the simulated GMs to the median spectrum (again in terms of MIDR) from the recorded GMs for each subset (as a function of the period and $\alpha$); similarly, Figure 11(b) shows the ratio of the log-standard deviations of the data in terms of MIDR from the simulated GMs to the standard deviation of the data (again in terms of log of MIDR) from the recorded GMs for each subset.

Figure 11 refers to systems with uniform stiffness distribution along the height (results for the other cases, not presented for the sake of brevity, confirm these findings). For the range of distances considered in this study ($5\,\text{km} < D < 52\,\text{km}$), ratios of the medians do not significantly change when computed from GMs ensembles, representative of different distance ranges for all the considered systems. Conversely, looking at the ratios of log-standard deviations for simulated and recorded GMs, moderate-period and long-period ordinates are significantly influenced by the distance range. In particular, the log-standard deviation of response to simulated records is larger than that of recorded ones across the period range 1–6 s. As discussed for the MIDR spectra of the Imperial Valley event (Figure 4), sensitivity of log-standard deviation of response to distance can be attributed to the presence of near fault effects (e.g., strong coherent velocity pulses) in the simulated dataset. To confirm this, it is worth noting that the Imperial Valley dataset features a total of 27 GMs all within 21 km from the



DOI: 10.1002/eqe

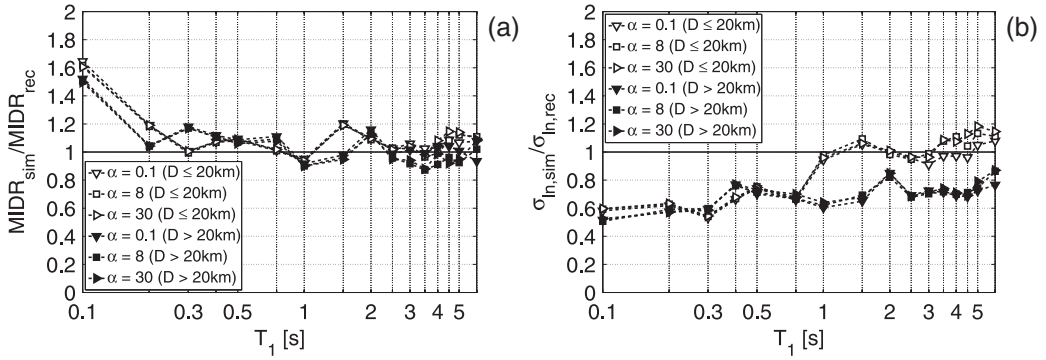


Figure 11. Effect of distance on the ratios of the medians (a) and log-standard deviations (b) of the generalized MIDR spectra for simulated GMs to the corresponding quantity computed for the recorded GMs (Northridge earthquake).

associated fault. Addressing near fault effects is the topic of current research; however, it is difficult to precisely quantify and/or calibrate these effects because of the scarcity of near-field recordings of moderate and large earthquakes. Insights from dynamic rupture simulations (e.g., [22]) have the potential to provide additional constraints on the characteristics of the rupture process used in the simulations. However, it is evident that strong directivity effects in the simulations require more study.

*3.4.2. Effect of site class.* Two subsets of 16 and 27 GMs representing two different $V_{S,30}$ ranges (in m/s), that is, $V_{S,30} < 400$ m/s and $V_{S,30} \geqslant 400$ m/s, are assembled from the datasets corresponding to the Northridge earthquake. Figure 12(a) shows the ratio of the median spectrum in terms of MIDR from the simulated GMs to the median spectrum (again in terms of MIDR) from the recorded GMs for each subset (as a function of the period); similarly, Figure 12(b) shows the ratio of the standard deviations of the data in terms of logs of MIDR from the simulated GMs to the standard deviation of the data (again in terms of logs of MIDR) from the recorded GMs for each subset (also in this case, we refer to the systems with uniform stiffness distribution along the height). For the range of $V_{S,30}$ considered in this study, ratios of the medians and standard deviations of the logs do not change significantly when computed from GM ensembles representative of different $V_{S,30}$ ranges for all the considered period and $\alpha$ values.

## 4. VALIDATION OF SIMULATED GMS USING NONLINEAR MDOF BUILDING SYSTEMS

The results presented in the previous sections shed light on the importance of considering the contribution of higher modes in the engineering validation of hybrid broadband GMs. However, the

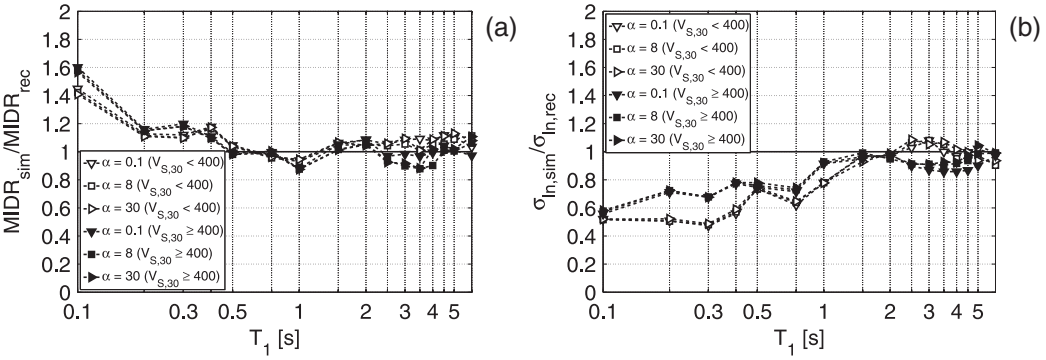


Figure 12. Effect of $V_{S,30}$ on the ratios of the medians (a) and log-standard deviations (b) of the generalized MIDR spectra for simulated GMs to the corresponding quantity computed for the recorded GMs (Northridge earthquake).



DOI: 10.1002/eqe

generalized MIDR analysis inherits some of the limitations and assumptions of modal analysis, such as assuming a linear elastic behavior. To alleviate this limitation, two nonlinear case study structures were considered. In particular, we are interested in moderate and long-period structures, where the comparisons presented in the previous sections in terms of spectral ordinates, generalized MIDR and floor acceleration spectra have not shown statistically significant differences in the seismic demands to simulated and recorded GMs. To investigate whether this conclusion holds in the case on inelastic response, a 6-story and a 20-story buildings with perimeter SMFs and designed for high seismic hazard under the 1994 UBC are considered here. These structures are selected because of the prevalence of this building type in the Los Angeles region, although they are not necessarily representative of all SMFs. The 6-story and the 20-story structures are denoted as U6 and U20, respectively. Details for the design of the structure can be found in [23].

### *4.1. Description of the structures and analytic models*

The finite element models of the considered structures are constructed by using the Open System for Earthquake Engineering Simulation (OpenSees) software (http://opensees.berkeley.edu/). In total, eight models are produced, with four variations on each of the two base structures. Two variations for the beam connection type are used, a brittle pre-Northridge connection and a ductile post-Northridge connection, denoted as 'preNR' and 'postNR', respectively. Additionally, two variations on the modeling strategy are implemented, a bare frame model, and a more robust model that consists of the bare frame model in all respects with addition of the gravity frame, denoted as '+GFL', as well as the slab contribution, denoted as '+MFS'. In the following, we will discuss the results for the (postNR + GFL + MFS) case; results for other buildings variations not shown herein lead to similar conclusions. The diaphragm of the structure is assumed to be rigid. Soil–structure–foundation interaction is not considered in the model, and the basement walls are not modeled; column bases are fixed. Lumped plasticity models are employed and attempted, to consider all significant contributions to the strength and stiffness of the structures as well as the cyclic deterioration of components. *P*–delta effects are included in the analysis, and 2.5% viscous damping is used in all modes of vibration. Further details can be found in [9].

Figure 13 shows the schematic configuration of the 6-story and 20-story moment frames. The structural components are elastic beam elements with plastic hinges at their ends and elastic column elements with *P–M* plastic hinges at their ends.

The geometries and spring properties of these components are varied according to the properties of the frames they represent. In particular, the moment frame connection type, whether pre-Northridge or post-Northridge, is considered in the plastic hinges of the moment frame beams. When the slab effect is modeled (+MFS), strength capacity of beam plastic hinges are increased. For models that included the gravity frame (+GFL), partially restrained rotation hinges are employed at the beam–column connections of gravity frame members. The effect of axial loading on column bending strength is incorporated in the models through *P–M* interaction. Table II shows the first-mode and second-mode periods of the structural systems used in this study. Further information on the modeling aspects of the 6-story and 20-story frames can be found in [9]. Although 3D models of the structures are built, the analysis is essentially 2D in that the GMs are applied along the building's transverse axis, parallel to the moment frames.

### *4.2. Results and discussions*

As discussed in Section 2, the model region for each event covers a wide area surrounding the fault, including many strong motion recording sites, in a large range of distances. In an effort to analyze structural response in the nonlinear range, only a limited number of these sites are used here in performing NLDA. To this aim, for each building, the value of the MIDR for each simulated record divided by the value of the MIDR for the corresponding recorded waveform (at the same station) is computed and plotted as a function of the ratio of the recorded spectral acceleration at the first period of the structure, $S_{a,rec}(T_1)$, divided by yield base shear coefficient $\gamma$. The latter is the ratio between the base shear at yielding point to the seismic weight of the structure. The base shear at yielding point is



DOI: 10.1002/eqe

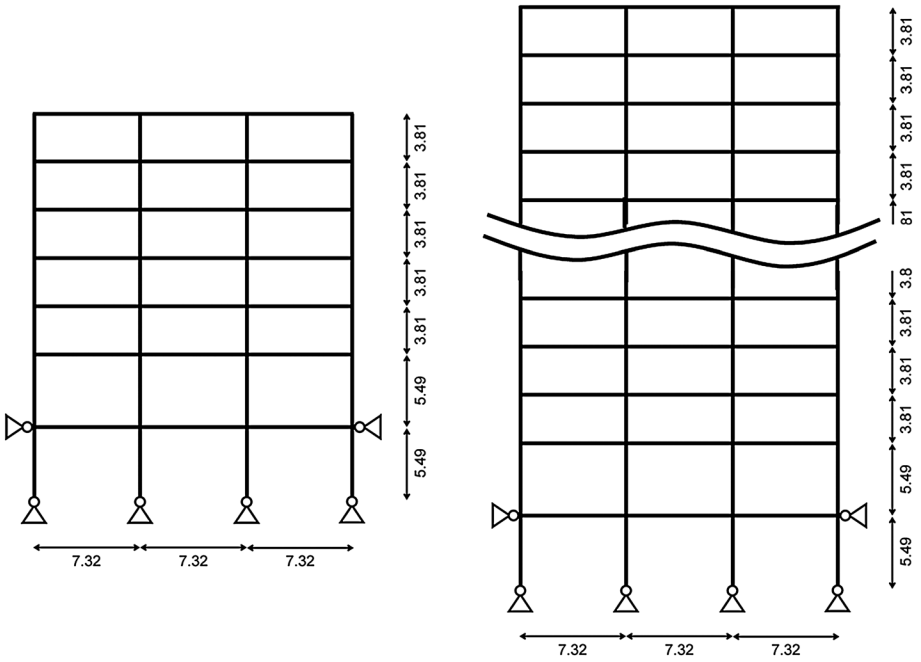


Figure 13. Elevations of the individual moment frames from the U20 and U6 structures (dimensions in meters).

Table II. Buildings periods.

| | Period (in direction of MF only) | |
|---|---|---|
| Structure name | $T_1$ (s) | $T_2$ (s) |
| U20 (postNR + GFL + MFS) | 3.683 | 1.265 |
| U6 (postNR + GFL + MFS) | 1.937 | 0.657 |

obtained from a pushover analysis performed with the load pattern described in [2] and the displacement control strategy (Figure 14).

Figure 15(a) refers to the U6 (postNR + GFL + MFS) building and Northridge event, whereas Figure 15(b) refers to the U20 (postNR + GFL + MFS) building (same event). This event has been selected because it is characterized by the largest number of stations; results for the other events are not shown to save space and similar observations can be drawn for these cases. One can assume that GMs characterized by $S_{a,rec}(T_1)/\gamma$ larger than unity has forced the structure into inelastic response.

For a subset of GMs with $S_{a,rec}(T_1)/\gamma \geqslant 1.0$, the median value of the time-peak IDR at a story level for the simulated records ($IDR_{sim}$) divided by the median value of IDR for the recorded dataset ($IDR_{rec}$) is plotted over the height of the building in Figure 16(a) (U6) and Figure 16(b) (U20). In the same figure, the ratio of the standard deviation of IDR (log of the data) for synthetic GMs divided by the standard deviation of IDR (log of the data) for recorded GMs is also plotted along the height of the building. In general, the median IDR profiles due to the simulated waveforms agree reasonably well with those due to the recorded GMs. In particular, for the U6 building subjected to the Northridge earthquake, the comparison between the median profiles for recorded and simulated GMs (Figure 16(a)) exhibits a technically zero bias along the height. Also, for the U20 building subjected to the Northridge earthquake, the bias is close to zero along the height (Figure 16(b)). These results are confirmed in terms of PFA (Figure 17), with a negligible bias along the height in terms of median response.

Figure 16 shows that the standard deviations of the log-IDR profiles produced by the simulated records are generally larger compared with those from the recorded GMs. This result is consistent



DOI: 10.1002/eqe

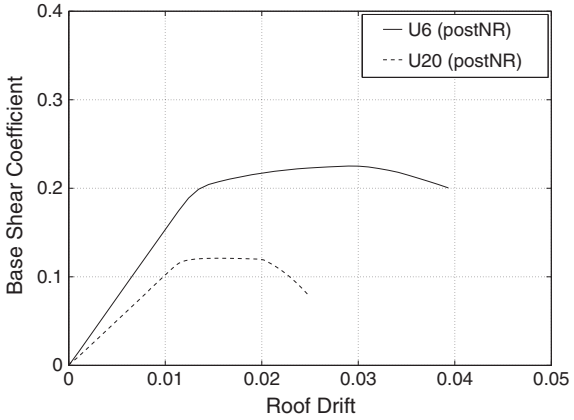


Figure 14. Pushover curves of the structures used in this study.

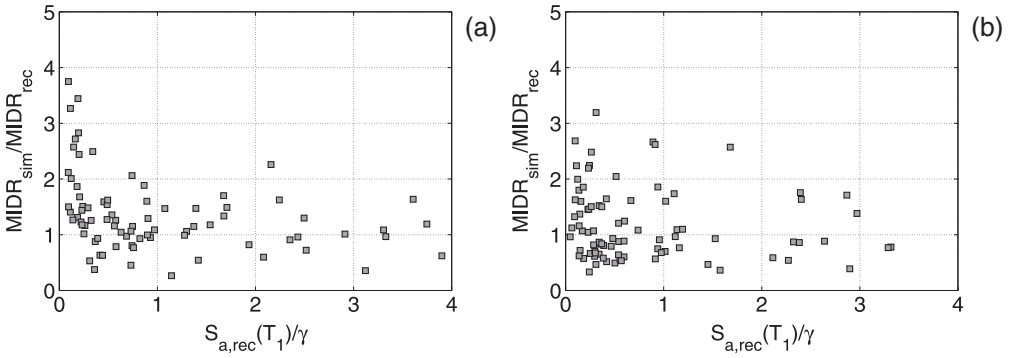


Figure 15. Ratios of the individual MIDR values for simulated GMs to the corresponding quantity computed for the recorded GMs as a function of $S_{\mathrm{a,rec}}(T_1)/\gamma$ for (a) U6 and (b) U20.

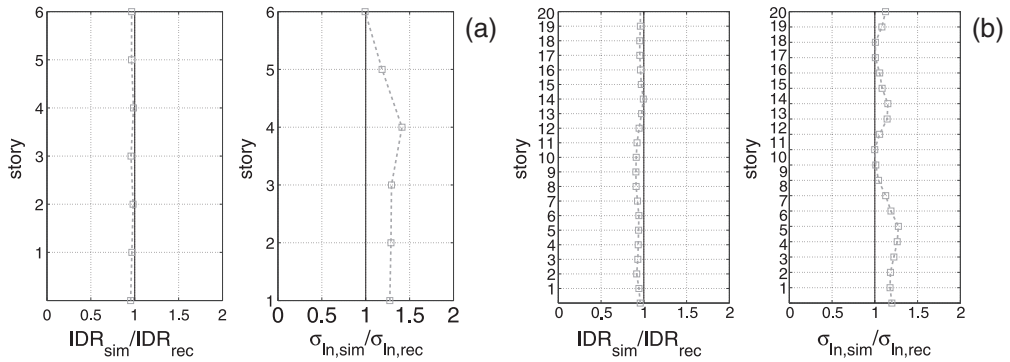


Figure 16. Ratios of the medians and log-standard deviations of IDR profiles for simulated GMs to the corresponding quantities computed for the recorded GMs for (a) U6 and (b) U20.

with the finding of Section 3.4.1 for the elastic response. In fact, the GMs for which the ratio $S_{\mathrm{a,rec}}(T_1)/\gamma$ is larger than unity are those characterized by short source-to-site distances and then, potentially, affected by forward directivity effects. However, hypothesis tests do not confirm these differences to be statistically significant, for both buildings and considered EDP.

The favorable comparisons shown for these two buildings lend further support to the predictive capabilities of the simulation methodology. However, the authors emphasize the fact that the observations and conclusions drawn here are based on a limited set of structures and further research is required to make more generalized conclusions.



DOI: 10.1002/eqe

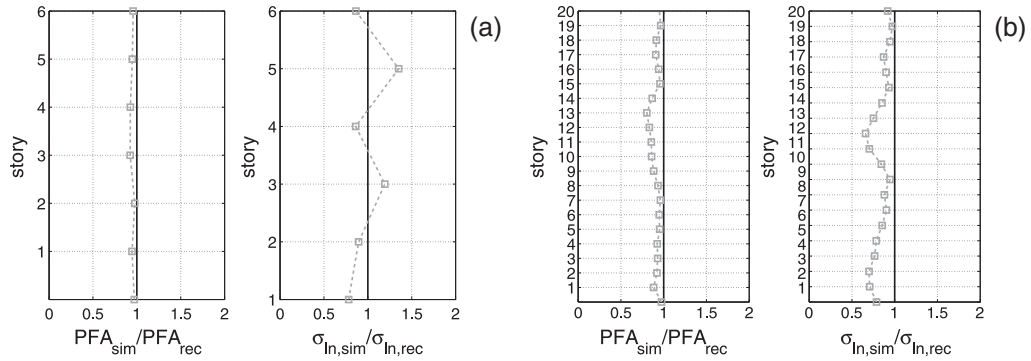


Figure 17. Ratios of the medians and log-standard deviations of PFA profiles for simulated GMs to the corresponding quantities computed for the recorded GMs for (a) U6 and (b) U20.

## 5. CONCLUSIONS

In recent years, significant progress has been made in modeling and simulation of broadband GMs suitable for both design and assessment of structures. The first part of this study investigated whether a state-of-the-art simulation technique produces generalized interstory drift and PFA spectra that are statistically distinguishable from those created by real records. The spectra are computed for elastic MDoF systems with periods ranging from 0.1 to 6 s and for different earthquake-resistant systems. The investigation is carried out by means of simulations for four historical earthquakes recorded at several stations located at various distances from the fault rupture, that is, the 1979 $M_w$ 6.5 Imperial Valley earthquake, 1989 $M_w$ 6.8 Loma Prieta earthquake, 1992 $M_w$ 7.2 Landers earthquake, and 1994 $M_w$ 6.7 Northridge earthquake. Results show that structural response estimated by using simulated records generally matches the response obtained using recorded motions. However, some differences exist between median estimate of seismic demand obtained by using real records and that obtained by simulations, especially in the short-period part of the spectra, where the simulation is semistochastic. The observed differences are due to systematic differences in the average shape around those periods of the elastic response spectra generated by synthetic and by real GMs. Moreover, the record-to-record variability of seismic demands produced by simulated and recorded GMs may be different, especially in the short-period range.

Using two case study structures, nonlinear IDR and PFA distributions over building height was studied; statistics are obtained and compared for both recorded and simulated time histories. These structures are SMFs designed for high seismic hazard, 20-story high-rise and 6-story low-rise buildings, similar to many SMFs structures in Los Angeles. Results of this analysis show that simulation matches well the inelastic demands produced by recorded GMs, at least for the cases made here.

Hypothesis tests are carried out with the aim of assessing quantitatively how significant the estimated biases can be. Tests have shown a statistical significance of the bias of simulated record in terms of maximum IDR and PFA only in the elastic case for short-period structures.

Finally, it is worth to remark that, although the study is mostly addressed to the engineering community, it may also provide insight for the simulations of earthquake records for engineering application.

ACKNOWLEDGEMENTS

This research was supported by *Rete dei Laboratori Universitari di Ingegneria Sismica* – ReLUIS for the research program founded by the Italian Department of Civil Protection – Executive Project 2010–2013, and the NSF and USGS sponsored Southern California Earthquake Center (SCEC). Their support is gratefully acknowledged. Any opinions, findings, and conclusions or recommendations expressed in this paper are those of the authors and do not necessarily reflect the views of the sponsors. Constructive and insightful comments and suggestions by two anonymous reviewers, Nicolas Luco and Brad Aagaard of USGS and Pierson Jones were very helpful in revising the paper.



DOI: 10.1002/eqe

REFERENCES


1. Bommer, JJ, Acevedo, AB. The use of real earthquake accelerograms as input to dynamic analysis, *Journal of Earthquake Engineering* 2004; **8**: S1, 43–91.
2. ASCE, American Society of Civil Engineering. Minimum Design Loads for Buildings and Other Structures (7-10), Standards ASCE/SEI 7-10. 2010.
3. Graves, RW, Pitarka A. Broadband ground-motion simulation using a hybrid approach. *Bulletin of the Seismological Society of America* 2010; **100**(5A): 2095–2123.
4. Iervolino I, Maddaloni G, Cosenza E. Eurocode 8 compliant real record sets for seismic analysis of structures. *Journal of Earthquake Engineering* 2008; **12**(1): 54–60.
5. Galasso, C, Zareian, F, Iervolino, I, Graves, RW. Validation of ground motion simulations for historical events using SDoF systems. *Bulletin of the Seismological Society of America* 2012; **102**(6): 2727–2740.
6. Miranda, E, Taghavi, S. Approximate floor acceleration demands in multistory building. I: formulation. *Journal of Structural Engineering, ASCE* 2005; **131**(2): 203–211.
7. Zareian, F, Krawinkler, H. Conceptual performance-based seismic design using building-level and story-level decision support system. *Earthquake Engineering & Structural Dynamics* 2012; **41**(11): 1439–1453. doi: 10.1002/eqe.2218.
8. Miranda, E. Approximate seismic lateral deformation demands in multistory buildings. *Journal of Structural Engineering, ASCE* 1999; **125**(4): 417–425.
9. Jones, P, Zareian, F. Relative safety of high-rise and low-rise steel moment-resisting frames in Los Angeles. *Structural Design of Tall Special Buildings* 2010; **19**(1-2): 183–196. doi: 10.1002/tal.559.
10. Iervolino I, De Luca F, Cosenza E. Spectral shape-based assessment of SDOF nonlinear response to real, adjusted and artificial accelerograms. *Engineering Structures* 2010; **32**(9): 2776–279.
11. Campbell, KW, Bozorgnia, Y. NGA ground motion model for the geometric mean horizontal component of PGA, PGV, PGD and 5% damped linear elastic response spectra for periods ranging from 0.01 to 10 s. *Earthquake Spectra* 2008; **24**(1): 139–171.
12. Graves, RW, Aagaard BT. Testing long-period ground-motion simulations of scenario earthquakes using the M w 7.2 El Mayor–Cucapah mainshock; evaluation of finite-fault rupture characterization and 3D seismic velocity models, *Bulletin of the Seismological Society of America* 2011; **101**(2): 895–907.
13. Miranda, E, Akkar, S. Generalized interstory drift demand spectrum. *Journal of Structural Engineering, ASCE* 2006; **132**(6), 840–852.
14. Miranda, E and Reyes, CJ. Approximate lateral drift demands in multi-story buildings with nonuniform stiffness. *Journal of Structural Engineering, ASCE* 2002; **128**(7): 840–849.
15. Star, L, Stewart, JP, Graves, RW. Comparison of ground motions from hybrid simulations to NGA prediction equations. *Earthquake Spectra* 2011; **27**(2): 331–350.
16. Seyhan, E, Stewart, JP, Graves, RW. Calibration of a semi stochastic procedure for simulating high frequency ground motions. *Earthquake Spectra* 2012; (accepted for publication).
17. Reinoso, E, Miranda, E. Estimation of floor acceleration demands in high-rise buildings during earthquakes. *The Structural Design of Tall and Special Buildings* 2005; **14**(2): 107–130.
18. Shapiro, SS, Wilk, MB. An analysis of variance test for normality (complete samples). *Biometrika* 1965; **52**(3-4): 591–611.
19. Welch, BL. The significance of the difference between two means when the population variances are unequal. *Biometrika* 1938; **29**: 350–362.
20. Satterthwaite, FE. Synthesis of variance. *Psychometrika* 1941; **6**(5): 309–316.
21. Mood, MA, Graybill FA, Boes DC. *Introduction to the Theory of Statistics* (3rd edition). McGraw-Hill Companies: New York, 1974.
22. Schmedes, J, Archuleta, RJ, Lavalle, D. Correlation of earthquake source parameters inferred from dynamic rupture simulations, *Journal of Geophysical Research* 2010; **115**: doi 10.1029/2009JB006689.
23. Hall JF. Seismic response of steel frame buildings to near-source ground motions. *Technical Report EERL 97-05*, California Institute of Technology, Pasadena, CA. 1997.




DOI: 10.1002/eqe